Published in final edited form as:
J Neurosci. 2012 February 1; 32(5): 1602–1611. doi:10.1523/JNEUROSCI.5601-11.2012.

LRRK2 Inhibition Attenuates Microglial Inflammatory Responses

Mark S. Moehle[1,4,5,#], **Philip J. Webber**[1,4,5,#], **Tonia Tse**[1,4], **Nour Sukar**[1,4], **David G. Standaert**[1,4], **Tara M. DeSilva**[2,4], **Rita M. Cowell**[3,4], and **Andrew B. West**[1,4,*]

[1]Department of Neurology, University of Alabama at Birmingham, Birmingham, Alabama 35294

[2]Department of Physical Medicine and Rehabilitation, University of Alabama at Birmingham, Birmingham, Alabama 35294

[3]Department of Psychiatry & Behavioral Neurobiology, University of Alabama at Birmingham, Birmingham, Alabama 35294

[4]Center for Neurodegeneration and Experimental Therapeutics, University of Alabama at Birmingham, Birmingham, Alabama 35294

[5]Neuroscience Graduate Program, University of Alabama at Birmingham, Birmingham, Alabama 35294

Abstract

Missense mutations in leucine-rich repeat kinase 2 (LRRK2) cause late-onset Parkinson disease, and common genetic variation in LRRK2 modifies susceptibility to Crohn disease and leprosy. High levels of LRRK2 expression in peripheral monocytes and macrophages suggest a role for LRRK2 in these cells, yet little is known about LRRK2 expression and function in immune cells of the brain. Here, we demonstrate a role for LRRK2 in mediating microglial pro-inflammatory responses and morphology. In a murine model of neuroinflammation, we observe robust induction of LRRK2 in microglia. Experiments with TLR4-stimulated rat primary microglia show that inflammation increases LRRK2 activity and expression while inhibition of LRRK2 kinase activity or knockdown of protein attenuates TNFα secretion and iNOS induction. LRRK2 inhibition blocks TLR4 stimulated microglial process outgrowth and impairs ADP stimulated microglial chemotaxis. However, actin inhibitors that phenocopy inhibition of process outgrowth and chemotaxis fail to modify TLR4 stimulation of TNFα secretion and iNOS induction, suggesting LRRK2 acts upstream of cytoskeleton control as a stress-responsive kinase. These data demonstrate LRRK2 in regulating responses in immune cells of the brain and further implicate microglial involvement in late-onset PD.

Introduction

The leucine rich repeat kinase 2 (LRRK2) gene was discovered as part of an evolutionarily conserved family of proteins marked by GTPase domains usually encoded together with kinase domains (Bosgraaf and Van Haastert, 2003). Missense mutations in both the kinase and GTPase domain in LRRK2 cause late-onset Parkinson Disease (PD) with clinical and pathological phenotypes nearly indistinguishable from idiopathic disease, possibly through the up-regulation of LRRK2 kinase activity (Paisan-Ruiz et al., 2004; Zimprich et al., 2004; West et al., 2005). Disease penetrance of LRRK2 mutations in PD is incomplete as lifetime risk in clinical populations is estimated at ~22–32%, suggesting strong modifiers of LRRK2

*Address correspondence to: Andrew West, 1719 6th Ave S., Birmingham, AL, 35226. Tel: 205 996 7697 Fax: 205 996 6580; abwest@uab.edu.
#These authors contributed equally to this work.

disease (Goldwurm et al., 2007). A modifying role for the immune system in PD susceptibility is supported by the association of the HLA region with late-onset disease (Hamza et al., 2011), and pathological studies of PD brains demonstrate strong microglial and T-cell activation and infiltration in susceptible brain nuclei (McGeer et al., 1988). Genome-wide association studies also highlight LRRK2 in modification of susceptibility to the chronic autoimmune Crohn disease and Mycobacterium leprae infection (Zhang et al., 2009; Umeno et al., 2011), raising the possibility that mutations in LRRK2 may modify immunogenic responses in PD.

LRRK2 is expressed in many different cell types in mammals but the intracellular function of LRRK2 is not clear. In the brain, LRRK2 is expressed in diverse neuronal subtypes and localizes to cytoskeletal structures and a variety of vesicular and membranous organelles (Biskup et al., 2006). In neurons, LRRK2 has been described as a potent regulator of the cytoskeleton where knockdown of protein enhances neurite outgrowth and mutant (overactive) LRRK2 expression inhibits outgrowth (MacLeod et al., 2006). LRRK2 may directly modify microtubule organization and the actin cytoskeleton through phosphorylation of substrates (Gillardon, 2009; Parisiadou et al., 2009). LRRK2 may also play additional kinase-dependent roles in the modification of synaptic vesicle storage and mobilization, in addition to kinase dependent roles in endocytosis, MAPK signaling, autophagy and apoptosis (Alegre-Abarrategui et al., 2009; Gloeckner et al., 2009; Piccoli et al., 2011).

Particularly high LRRK2 expression has been recently discovered in macrophage and monocytic cells, but not T cells, leading to speculation of a functional role for LRRK2 in the innate immune system (Thevenet et al., 2011). A number of powerful tools, including highly-specific rabbit monoclonal LRRK2 antibodies and potent and selective LRRK2 small molecule kinase inhibitors, have become available that allow for a careful dissection of LRRK2 function in cells of the immune system. Based on the expression of LRRK2 in monocytes, we hypothesized a role for LRRK2 in the immune cells of the brain. Our results show that LRRK2 is expressed in activated microglia and that LRRK2 modulates pro-inflammatory responses in these cells. Alterations in LRRK2 function may modify inflammatory responses in neurodegenerative and infectious diseases, potentially leading to disease initiation or modification of progression.

Methods

Immunohistochemistry and Immunofluorescence

Male 8–12 week old WT or LRRK2 KO C57BL6/J mice (provided by Heather Melrose) or Tg(TH-eGFP)DJ76Gsat were perfused with room temperature (RT) phosphate buffered saline solution (PBS, pH 7.4), then 4% paraformaldehyde (PFA) in PBS, and brains removed and post-fixed in 4% PFA in PBS at 4°C for 12 hours with agitation, then embedded in 30% sucrose/PBS for 24 hours at 4°C, then frozen in isopentane and sectioned at 40 μm width on a freezing microtome. Freshly cut sections were rinsed and immediately treated with 0.3% H_20_2 in methanol for 30 min at RT with mild agitation, rinsed and treated with 10 mM Na-Citrate, pH 6.0, 0.05% tween, for 30 min at 37°C. Sections were rinsed and blocked first in 3% non-fat milk in PBS with 0.3% triton x-100 for 1 hour RT and then in 10% normal goat serum in PBS with 0.3% triton x-100 for one hour. LRRK2 antibody solution (containing 0.2 μg/mL for DAB or 1 μg/mL for immunofluorescence rabbit monoclonal C-41, Epitomics, 5% goat serum, 0.1% triton x-100, and 0.01% sodium azide) was applied to sections for 24 hours at 4°C with mild agitation. Sections were rinsed and Goat Anti-Rabbit:biotin (Vector labs), Goat Anti-Rabbit DyLight 649 (Jackson Laboratories), Isolectin-B4:FITC or Isolectin-B4:Biotin (Sigma), was added (as indicated) for 24 hours at 4°C. Sections for immunofluorescence were mounted with ProLong Gold

(Invitrogen) onto coverslips. Sections with biotinylated markers were developed with the Vectastain Elite ABC kit and Impact DAB (Vector labs) according to manufacturer's recommendations.

LPS injections

5 μg of LPS (15k endotoxin units, Sigma) was stereotactically injected in 1 μL volume with a flow rate of 0.2 μL/min using a NanoMite pump (Harvard Apparatus) fitted with a 32 gauge fully beveled needle and gas-tight syringe (Hamilton), with a 5 min wait for needle withdrawal, in mice anesthetized with isoflurane. Coordinates were −3.4 AP, −1.1 ML, and −3.9 DV for SNpc and +0.4 AP, −1.5 ML, and −2.5 DV for striatum, with respect to Bregma. For LRRK2 activity assays, FLAG-LRRK2 BAC mice (Jackson strain #012466) were utilized, and FLAG-M2 resin (Sigma) was utilized according to manufacturer's recommendations to immunoprecipitate LRRK2 protein. Animal usage was institutionally approved.

Western blotting, ELISA, and chemicals

Antibodies to LRRK2 (Epitomics, clone C-41), β-actin, GFAP, MBP (Sigma), CD-68 (Serotec), MAP2 (Millipore), GAPDH, IRF-1, VDAC (Santa Cruz), iNOS, Phospho-p38, Ikk-α (Cell Signaling) were used according to manufacturer's suggestions. Antibodies to pT1503 were previously described, and were combined with de-phosphopeptide at a concentration of 10 μg/ml during antibody incubations (Webber et al., 2011). Rat TNFα ELISA assays were from eBioscience. Sunitinib (LC Labs), L2In1 (provided by Dario Alessi), and cytochalasin D (Sigma) were dissolved at a concentration of 10 mM in DMSO. DMSO controls represent DMSO concentrations present at the highest amount in the experiment, and did not exceed 0.04% in any experiment.

Quantitative RT-PCR

Total RNA was extracted with Trizol reagent (Invitrogen) and first strand cDNA generated with Superscript III (Invitrogen). qPCR was performed using Taqman assays Rn01455646_m1 TBP and Rn00562055_m1 TNFα primer sets (Invitrogen) and iQ Powermix (Bio-rad). Thermocycling was performed on a Bio-rad CFX96 machine.

LRRK2 kinase assays

Kinase assays were performed as previously described (Sen et al., 2009). Recombinant purified human LRRK2 (Invitrogen) was combined into kinase buffer with LRRKtide substrate (Enzo Bioscience) and activity measured by scintillation counting of P-81 Whatman phosphocellulose paper.

Lentiviral Purification

Lentivirus preparation was performed as previously described (Tomlinson, 2008). HEK293-FT cells were transfected with pLP1, pLP2, pVSV-G and lentiviral expression vectors pLKO.1_LRRK2 (Plasmid # TRCN0000022655, shRNA-A, and #TRCN0000022658 , shRNA-B, Open Biosystems), or pLKO.1_Non-coding (NC) shRNA (Addgene plasmid 1864, courtesy of David Sabatini), or cFUGW (no RNAi) control. For determination of titer, RNA was extracted and cDNA was synthesized using the SuperScript VILO cDNA synthesis kit (Invitrogen). Real time PCR reaction was performed using primers that target the RRE element (F-GCA GCA GGA AGC ACT ATG; R-CGC CTC AAT AGC CCT CAG C). Ct values obtained from the virus were compared to the plasmid standard curve in order to determine the number of copies of virus/ μL. eGFP epifluorescence was used to verify that >90% of cells were transduced for the entirety of the experiment.

Primary microglia cell cultures

Primary mixed glial cultures were isolated from the forebrains of 2-day old Swiss Webster rats of either sex using a differential detachment method. Forebrains were digested with Hank's Balanced Salt Solution (Gibco) containing 0.01% trypsin and 10 μg/ml DNase and triturated with DMEM (Invitrogen) containing 20% heat-inactivated fetal bovine serum (FBS, Hyclone) and 1% penicillin–streptomycin. The dissociated cell suspension was plated onto poly-D-lysine-coated flasks. Media changes with DMEM containing 20% fetal bovine serum and 1% penicillin-streptomycin were performed every other day for 7 days. Microglia were separated by shaking the flasks for 1 hour at 200 RPM. The resulting microglial cell suspension was removed and plated at a density of ~1×10^5 cells/cm^2 in DMEM supplemented with 10% FBS and 10 ng/mL GM-CSF (Peprotech). The purity of microglia was verified by anti-rat CD-68 (Serotec) immunolabeling and western blot.

Morphological assessment

Randomized captured phase contrast images were derived from live cultures in a 37°C humidified chamber at 5% CO_2 on a Carl Ziess Cell Observer using Axiovision 4.7 Mark and Find controller. Prior to image collection, cells were incubated with 2.5 μM propidium iodide and 10 μM Hoechst 33342 for 10 min. Resultant images were analyzed by an observer blinded to experimental identity using ImageJ software to calculate process length in microglia cells.

Chemotaxis assay

90,000 primary microglia cells were added to transwell plates (8 μm pore, 24-well inserts, Corning) immediately after microglial removal from astrocyte beds, and allowed to adhere to the upper chamber for 6 hours. The lower chamber was then supplemented with 100 μM ADP (Sigma) to encourage migration through the membrane to the lower chamber, and experimental drug or DMSO was added to both the upper and lower chamber. After 30 additional hours, media was removed and the total number of cells counted, after an incubation with 10 μM Hoechst 33342 for 10 min, on a Carl Zeiss Cell Observer using Mark and Find software.

Statistics

Data from all experiments were analyzed with GraphPad Prism and InStat software.

Results

LRRK2 expression in TLR4-activated microglia

High LRRK2 expression in peripheral mouse monocytes and macrophages led us to examine whether LRRK2 may be expressed in brain resident macrophage cells (*i.e.*, microglia). We first applied recently characterized and highly specific rabbit monoclonal antibodies directed against LRRK2 to normal mouse brain tissue and failed to detect any cells positive for LRRK2 with morphology consistent with microglia, despite strong LRRK2 immunoreactivity in several neuronal populations. Since LRRK2 has been hypothesized as a stress-responsive kinase, we analyzed brain tissue from mice subjected to an intracranial injection of the potent toll-like receptor 4 (TLR4) agonist lipopolysaccharide (LPS) for a period of 24 hours. Although we observed no loss of tyrosine hydroxylase (TH) positive cells at this time point, the intensity of TH expression was slightly diminished (Figure 1A–C). Whereas only blood vessels were labeled by isolectin B4 in the contralateral side to LPS injection (Figure 1D), numerous small strongly stained cells consistent with activated microglia were detected in the LPS treated SNpc (Figure 1E–F). LRRK2 staining in the LPS injected SNpc revealed a strong induction of LRRK2 immunoreactivity in small cells with a

morphology and size consistent with the activated microglia identified by isolectin B4 (Figure 1H). This staining was abolished in LRRK2 knockout mice (Figure 1I). LRRK2 protein was undetectable in white matter tracts in normal brain tissue, although many LRRK2-positive small cells were found in the corpus callosum of mice after an intrastriatal LPS injection (Figure 1K). To rule out non-specific or cross-reactive labeling, non-immune rabbit IgG was also applied at comparable concentrations to LRRK2 antibody treated sections; negligible immunoreactivity was observed in these negative control sections and none reminiscent of microglia cells. Finally, staining in LRRK2 KO mice revealed the LRRK2 monoclonal antibody to be specific for LRRK2 (Figure 1I, L).

To co-localize LRRK2 with microglial markers in TLR4-activated microglia, a triple staining protocol that utilizes a single fluorescently labeled antibody was developed and applied to mice LPS-treated in either the SNpc or striatum (Figure 2). 24 hours post-injection, microglial cells rapidly accumulated and surrounded TH positive neurons (Figure 2A). Microglia could not be detected in the SNpc in animals that did not receive an LPS injection (Figure 2B). Similar to the SNpc, LRRK2 co-localized to microglial cells present in the white-matter tract post-striatal LPS injection (Figure 2C). Resident microglia with resting morphologies in non-injected animals failed to demonstrate immunoreactivity for LRRK2 (Figure 2D). As in Figure 1, whole-rabbit IgG control stained sections confirmed specificity of staining, and the LRRK2 antibody produces a single band of the correct size on western blot analysis (Figure 2E).

LRRK2 induction in TLR4-stimulated cells

TLR4 activation stimulates signal transduction pathways responsible for the up-regulation of pro-inflammatory factors. To further explore LRRK2 activity in response to TLR4 stimulation, mice transgenic for a FLAG-LRRK2 BAC insert were injected (bilateral) with LPS in the SNpc and the SNpc and immediately surrounding regions were removed after 24 hours. After LRRK2 immunoprecipitation from this tissue, LRRK2 was allowed to autophosphorylate for 15 min in the presence of 100 μM ATP, and protein eluted and transferred to membranes and probed with the recently described autophosphorylation specific antibody pT1503 (Webber et al., 2011). LPS treatment significantly increased the proportion of LRRK2 in an activated state as revealed by an enhanced proportion of autophosphorylated LRRK2 (Figure 2B). To ensure the pT1503 antibody could not cross-react with non-autophosphorylated LRRK2 protein, recombinant protein harboring mutations in the 1503 autophosphoraytion site or in the kinase domain (kinase dead, D1994A) was derived from transiently transfected cells and evaluated by western blot (Figure 2C). The pT1503 antibody could not detect signal in the kinase dead or the T1503A mutant LRRK2 protein, suggesting a high degree of specificity for this antibody.

To address whether LRRK2 expression also becomes up-regulated during TLR4 activation, primary microglia in culture were treated with increasing concentrations of LPS for 12 hours and LRRK2 protein levels determined by western blot (Figure 3E). 100 ng/mL of LPS was sufficient to increase levels of LRRK2 protein obtained in SDS-solubilized cell lysates, while higher concentrations of LPS failed to further increase LRRK2 induction. These primary microglia cultures were free from other cell types and >99% of cells in culture were CD-68 positive (data not shown). Quantification of LRRK2 protein levels across primary microglia, astrocytes, hippocampal neurons and oligodendrocytes, all derived from post-natal day 2 rats, unexpectedly revealed LRRK2 expression in primary astrocytes despite the lack of expression we could observe in these cells *in vivo*. LRRK2 expression in primary microglia cells is comparable to that of primary neurons in culture (Figure 3D).

We next determined whether LRRK2 expression is up-regulated at the mRNA level but failed to detect any significant differences after 12 hours of induction with various doses of

LPS, suggesting important post-transcriptional regulation of LRRK2 in microglia (Figure 3G). LRRK2 distribution by immunofluorescence in primary microglia is consistent with that of previous reports with strong perinuclear staining and nuclear exclusion, both in non-LPS and LPS treated microglia (Figure 3H). LRRK2 expression in human derived cells of monocytic and microglia origin appears to be conserved (Figure 3I), with similar LRRK2 up-regulation in THP-1 cells treated with LPS. Quantitative PCR analysis for LRRK2 mRNA also revealed no significant changes in LRRK2 levels in these cells, despite strong up-regulation of LRRK2 protein levels (Figure 3K and data not shown).

Inhibition of LRRK2 kinase activity attenuates pro-inflammatory microglial signaling

A post-transcriptional induction of LRRK2 and enhanced autophosphorylation in purified protein suggests possible involvement of LRRK2 during a pro-inflammatory response. We first evaluated the inhibitory potential of the two most potent and specific LRRK2 inhibitors yet described, L2in1 and Sunitinib, under common conditions. We derived IC_{50} values of 40.3 and 126.4 nM under uniform conditions, respectively, demonstrating L2in1 as more potent against LRRK2 kinase activity *in vitro* (Figure 4A,B). Sunitinib inhibits with similar potency several receptor tyrosine kinases including the platelet-derived growth factor receptor (PDGF-R) and vascular endothelial growth factor receptor (VEGFR) in addition to LRRK2, and L2in1 is highly specific for LRRK2 but is predicted to inhibit several other kinases including MAPK7 and Aurora-A (Dzamko et al., 2011). However, neither small molecule inhibits any known kinases that obviously link to TLR4 receptor signaling when applied at nanomolar or low micromolar concentrations. In addition, both inhibitors are structurally distinct from one another and there is no common off-targets known.

Secretion of the pro-inflammatory cytokine TNFα by microglia may represent a major modifier of neurotoxicity in models of Parkinson disease (Harms et al., 2011). Pre-treatment of microglia with nanomolar concentrations of either L2in1 or Sunitinib significantly attenuated the release and transcriptional induction of TNFα in primary cultured microglia (Figure 4D, E). iNOS and p38 are both critical targets of TNFα and effectors of continued TNFα release in autocrine signaling. In agreement with an attenuated inflammatory response to TLR4 stimulation, significantly reduced levels of iNOS induction and phosphorylated p38 were observed 6 hours post-LPS treatment (Figure 5F, G). To our knowledge, this is the first demonstration of anti-inflammatory activity for either small molecule LRRK2 inhibitor.

To determine whether removal of total LRRK2 protein produces effects comparable to acute kinase inhibition, we developed lentivirus capable of knocking down LRRK2 expression in primary microglia (Figure 5B). Lentivirus has previously been described as an effective method to genetically modify primary microglia without adverse effects on inflammatory responses (Balcaitis et al., 2005). To knockdown LRRK2 by RNAi in microglia, highly purified lentivirus was applied in increasing concentrations to determine the minimum amount of virus required to knockdown ~90% of LRRK2 protein. Control shRNA (non-coding, NC) lentivirus was also applied at identical concentrations and no adverse toxic or inflammatory effects on the microglia were observed. Knockdown of LRRK2 was sufficient to reduce TNFα secretion similar to LRRK2 kinase inhibition via small molecule inhibitor exposure (Figure 5C). LRRK2 knockdown also inhibited TLR4-mediated iNOS induction (Figure 6D, E). Phosphorylation of p38 was unchanged by LRRK2 RNAi, although basal levels of phospho-p38 rose to the levels of post-LPS phospho-p38 as a consequence of the extended *in vitro* culture period required for LRRK2 protein knockdown (Figure 6D). Collectively, these results suggest that LRRK2 kinase activity and expression are required for a full inflammatory response in microglia.

LRRK2 kinase activity is required for microglial morphological remodeling during activation

Microglia initially respond to LPS and other pro-inflammatory factors by extending processes into the environment (Sheng et al., 2011), with eventual (>12 hours) retraction into a classic activated amoeboid morphology as autocrine effects contribute to a positive feedback loop in pure microglial cultures. We noticed that in the presence of LRRK2 inhibitors or LRRK2 shRNA, LPS treatment failed to cause any significant morphological differences from non-LPS treated controls (Figure 6). This failure to morphologically respond to LPS was not due to an enhanced rate of cell death since Hoechst and propidium iodide staining revealed comparable results across conditions.

Microglial dynamic fine process extension have been suggested to play a critical role in mediating responses to local brain injury and stressors (Davalos et al., 2005). Because of migroglial dependence on LRRK2 for mediating a morphological response to LPS, we hypothesized that a chemotactic response to the potent microglial chemoattractant ADP may likewise be compromised in the absence of LRRK2 activity. Microglial cells immediately plated onto transwell permeable membranes after removal from astrocyte cultures demonstrated reduced migration to the bottom-well in the presence of LRRK2 inhibitors (Figure 7). An actin inhibitor cytochalasin D nearly abolished migration of microglia through the membrane, demonstrating the importance of cytoskeleton architecture in this process.

Since inhibition of LRRK2 has been shown to modify intracellular cytoskeleton architecture and process outgrowth in neurons (MacLeod et al., 2006), we reasoned that LRRK2 inhibition of process outgrowth and chemotaxis may link LRRK2 action, albeit indirectly, to anti-inflammatory activities. To test this hypothesis, we applied the actin inhibitor cytochalasin D to repress LPS-induced morphological remodeling. A 2 μM concentration of cytochalasin D was sufficient to phenocopy LRRK2 in preventing LPS induced process extension, although as opposed to LRRK2 inhibition, cytochalasin D also reduced normal process morphology in non-LPS treated microglia (Figure 8B). Surprisingly, cytochalasin D failed to demonstrate any anti-inflammatory activity; rather, TNFα secretion was positively regulated although we were not able to detect an overall change in iNOS induction (Figure 8C–D). We conclude that LRRK2 dependent morphological changes are a result of upstream LRRK2-dependent anti-inflammatory signaling. Disruption of LRRK2 activity thus prevents a full inflammatory response in these cells that is reflected both morphologically, by TNFα secretion, and by iNOS induction.

Discussion

Genetic studies unambiguously tie LRRK2 to several human diseases. Most notably, high frequencies of causative pathological mutations have been identified in late onset PD. Whole genome association studies pinpoint LRRK2 as one of a few genes where common genetic variability underlies susceptibility to leprosy and Crohn's disease, highlighting a potential immunologic function for LRRK2. Other evidence also suggests that immune function is involved in the pathogenesis of PD, since genetic variation in the HLA region associates with PD (Hamza et al., 2011), and numerous pathologic studies describe microglia activation in PD. LRRK2 appears to be expressed in cells of the innate but not adaptive immune system. A recent study demonstrated that the expression of LRRK2 in cultured bone marrow- derived macrophages from mice is up regulated in response to LPS (Hakimi et al., 2011). Another recent study demonstrated that LRRK2 expression is also stimulated by the IFN-γ response in peripheral blood mononuclear cells (Gardet et al., 2010). Thus, it has been hypothesized that LRRK2 may mediate some aspect of signaling or differentiation in innate immune cells.

The recent development of highly specific and sensitive rabbit monoclonal LRRK2 antibodies and LRRK2 knockout mice enables immunohistochemistry studies with a higher degree of confidence. Our results show that in brain tissue challenged with the potent TLR4 agonist LPS, LRRK2 expression is induced in activated microglia. Immunoprecipitation of LRRK2 protein from brains treated with LPS revealed enhanced levels autophosphorylation, which implies greater LRRK2 activity. Direct demonstration of enhanced LRRK2 enzyme activity in neuroinflammation awaits the identification of bone fide LRRK2 kinase substrates. Interestingly, we found that the accumulation of LRRK2 protein which occurs during inflammatory signaling in primary microglia is not accompanied by significant changes in mRNA levels, suggesting important post-transcriptional regulation.

We find that inhibition of LRRK2, either by small molecule kinase inhibitors or RNAi knockdown, attenuates pro-inflammatory signaling in response to TLR4 activation. LRRK2 is hierarchically clustered in the tyrosine-kinase like superfamily nearby kinases important for inflammatory signaling in immune activation, such as the Interleukin-1 receptor associated kinase (IRAK) family and the mixed lineage kinase (MLK) family (West et al., 2007). Thus, we hypothesized that LRRK2 may function as a stress response kinase during a neuroinflammatory stimulus in the brain by facilitating signal transduction pathways in affected cells. We utilized two approaches to dissect the role of LRRK2 in TLR4 mediated inflammatory responses in primary microglia: small molecule inhibition and RNAi knockdown of total protein. While a single inhibitory molecule may be confounded by off target effects, we find agreement with multiple effective molecules that are unlikely to have over lapping off targets. In cultured rat microglia, peak TNFα release was observed 6 hours post LPS exposure and reduced by 12 hours, and in the context of LRRK2 inhibition, peak induction was reduced by greater than 20% by either LRRK2 small molecule inhibition or RNAi. Likewise, reduced levels of the TNFα target iNOS were detected by western blot. Although this effect is modest in the overall pro-inflammatory response, a cumulative effect over time may link this modifying effect with susceptibility to neurodegeneration since both TNFα and iNOS have been implicated as critical determinants of neurotoxicity.

We also observed an effect of LRRK2 inhibition on the morphological response of microglia to LPS. Exposure of microglia to LPS in the context of inhibited LRRK2 prevents the normal morphological response of fine process extension and cytoskeleton remodeling. The functional role for microglial fine process extension during initial phases of inflammatory signaling are not clear, but may involve physical sequestration of infiltrating pathogens *in vivo* in damaged areas by providing a network blockage (Davalos et al., 2005). We hypothesized that inhibition of fine process extension during LPS stimulation may itself have an anti-inflammatory effect due to negative effects on receptor clustering and lipid raft shuttling. Although actin inhibition nearly abolished fine process extension, there were no anti-inflammatory effects observed. We therefore conclude that a full pro-inflammatory response mediates process extension, but process extension itself does not mediate pro-inflammatory signaling. Thus, LRRK2 inhibition may prevent a full inflammatory response required for fine-process extension, placing LRRK2 as an upstream stress-responsive kinase to TLR4 activation.

Although the current data would suggest an overall pro-inflammatory role for LRRK2, given the complexity of neuroinflammation and the limitations of interpreting microglial action in purified cultures *in vitro*, it is possible an overall anti-inflammatory role for LRRK2 may be likewise envisaged. Indeed, we find that LRRK2 inhibitors quell a chemotaxic response to the potent microglial chemoattractant ADP. However, we interpret these results with some caution since we were not able to perform comparable experiments under conditions of LRRK2 RNAi. In these experiments, it was not possible to remove microglia already transduced with lentiviral LRRK2 shRNA molecules, incubated for the time required to

knockdown LRRK2 protein, without killing the microglia cells. Besides microglia, LRRK2 may also be expressed in anti-inflammatory IL-10 producing macrophages in the brain, and inhibition of LRRK2 in these cells may mitigate anti-inflammatory signaling. Transgenic and LRRK2 knockout mice can be utilized in future studies to clarify overall effects of LRRK2 in neuroinflammation.

In this study, we contribute to a growing body of evidence that suggests a possible modifying role for the immune system and inflammation in PD by demonstrating LRRK2 activation in microglia and critical function in pro-inflammatory responses. It seems hypothetically possible that activating mutations in LRRK2, such as the G2019S missense mutation in the kinase activation loop, may serve to exaggerate neuroinflammatory responses that predispose to neurodegeneration susceptibility in PD. Further studies with *in vivo* models of neuroinflammation and associated neurodegeneration are warranted and will be critical to address the pathophysiological function of LRRK2.

Acknowledgments

This work was supported by the Michael J. Fox Foundation for Parkinson's Research, the American Parkinson's Disease Association, the National Institutes of Health R01-NS064934, UAB Neuroscience Core Center NS047466 and the benevolence of John A. and Ruth R Jurenko. M.S.M. is supported by T32 NS061788. The authors wish to thank Dario Alessi for L2in1 compound, Bassel Sawaya for purified human microglia cells, and Heather Melrose and Matthew Farrer for LRRK2 knockout mice.

Reference List

Alegre-Abarrategui J, Christian H, Lufino MM, Mutihac R, Venda LL, Ansorge O, Wade-Martins R. LRRK2 regulates autophagic activity and localizes to specific membrane microdomains in a novel human genomic reporter cellular model. Hum Mol Genet. 2009; 18:4022–4034. [PubMed: 19640926]

Balcaitis S, Weinstein JR, Li S, Chamberlain JS, Moller T. Lentiviral transduction of microglial cells. Glia. 2005; 50:48–55. [PubMed: 15625717]

Biskup S, Moore DJ, Celsi F, Higashi S, West AB, Andrabi SA, Kurkinen K, Yu SW, Savitt JM, Waldvogel HJ, Faull RL, Emson PC, Torp R, Ottersen OP, Dawson TM, Dawson VL. Localization of LRRK2 to membranous and vesicular structures in mammalian brain. Ann Neurol. 2006; 60:557–569. [PubMed: 17120249]

Bosgraaf L, Van Haastert PJ. Roc, a Ras/GTPase domain in complex proteins. Biochim Biophys Acta. 2003; 1643:5–10. [PubMed: 14654223]

Davalos D, Grutzendler J, Yang G, Kim JV, Zuo Y, Jung S, Littman DR, Dustin ML, Gan WB. ATP mediates rapid microglial response to local brain injury in vivo. Nat Neurosci. 2005; 8:752–758. [PubMed: 15895084]

Dzamko N, Deak M, Hentati F, Reith AD, Prescott AR, Alessi DR, Nichols RJ. Inhibition of LRRK2 kinase activity leads to dephosphorylation of Ser(910)/Ser(935), disruption of 14-3-3 binding and altered cytoplasmic localization. Biochem J. 2011; 430:405–413. [PubMed: 20659021]

Gardet A, Benita Y, Li C, Sands BE, Ballester I, Stevens C, Korzenik JR, Rioux JD, Daly MJ, Xavier RJ, Podolsky DK. LRRK2 is involved in the IFN-gamma response and host response to pathogens. J Immunol. 2010; 185:5577–5585. [PubMed: 20921534]

Gillardon F. Leucine-rich repeat kinase 2 phosphorylates brain tubulin-beta isoforms and modulates microtubule stability--a point of convergence in parkinsonian neurodegeneration? J Neurochem. 2009; 110:1514–1522. [PubMed: 19545277]

Gloeckner CJ, Schumacher A, Boldt K, Ueffing M. The Parkinson disease-associated protein kinase LRRK2 exhibits MAPKKK activity and phosphorylates MKK3/6 and MKK4/7, in vitro. J Neurochem. 2009; 109:959–968. [PubMed: 19302196]

Goldwurm S, Zini M, Mariani L, Tesei S, Miceli R, Sironi F, Clementi M, Bonifati V, Pezzoli G. Evaluation of LRRK2 G2019S penetrance: relevance for genetic counseling in Parkinson disease. Neurology. 2007; 68:1141–1143. [PubMed: 17215492]

Hakimi M, Selvanantham T, Swinton E, Padmore RF, Tong Y, Kabbach G, Venderova K, Girardin SE, Bulman DE, Scherzer CR, LaVoie MJ, Gris D, Park DS, Angel JB, Shen J, Philpott DJ, Schlossmacher MG. Parkinson's disease-linked LRRK2 is expressed in circulating and tissue immune cells and upregulated following recognition of microbial structures. J Neural Transm. 2011; 118:795–808. [PubMed: 21552986]

Hamza TH, Zabetian CP, Tenesa A, Laederach A, Montimurro J, Yearout D, Kay DM, Doheny KF, Paschall J, Pugh E, Kusel VI, Collura R, Roberts J, Griffith A, Samii A, Scott WK, Nutt J, Factor SA, Payami H. Common genetic variation in the HLA region is associated with late-onset sporadic Parkinson's disease. Nat Genet. 2011; 42:781–785. [PubMed: 20711177]

Harms AS, Barnum CJ, Ruhn KA, Varghese S, Trevino I, Blesch A, Tansey MG. Delayed dominant-negative TNF gene therapy halts progressive loss of nigral dopaminergic neurons in a rat model of Parkinson's disease. Mol Ther. 2011; 19:46–52. [PubMed: 20959812]

MacLeod D, Dowman J, Hammond R, Leete T, Inoue K, Abeliovich A. The familial Parkinsonism gene LRRK2 regulates neurite process morphology. Neuron. 2006; 52:587–593. [PubMed: 17114044]

McGeer PL, Itagaki S, Boyes BE, McGeer EG. Reactive microglia are positive for HLA-DR in the substantia nigra of Parkinson's and Alzheimer's disease brains. Neurology. 1988; 38:1285–1291. [PubMed: 3399080]

Paisan-Ruiz C, et al. Cloning of the gene containing mutations that cause PARK8-linked Parkinson's disease. Neuron. 2004; 44:595–600. [PubMed: 15541308]

Parisiadou L, Xie C, Cho HJ, Lin X, Gu XL, Long CX, Lobbestael E, Baekelandt V, Taymans JM, Sun L, Cai H. Phosphorylation of ezrin/radixin/moesin proteins by LRRK2 promotes the rearrangement of actin cytoskeleton in neuronal morphogenesis. J Neurosci. 2009; 29:13971–13980. [PubMed: 19890007]

Piccoli G, Condliffe SB, Bauer M, Giesert F, Boldt K, De Astis S, Meixner A, Sarioglu H, Vogt-Weisenhorn DM, Wurst W, Gloeckner CJ, Matteoli M, Sala C, Ueffing M. LRRK2 controls synaptic vesicle storage and mobilization within the recycling pool. J Neurosci. 2011; 31:2225–2237. [PubMed: 21307259]

Sen S, Webber PJ, West AB. Dependence of leucine-rich repeat kinase 2 (LRRK2) kinase activity on dimerization. J Biol Chem. 2009; 284:36346–36356. [PubMed: 19826009]

Sheng W, Zong Y, Mohammad A, Ajit D, Cui J, Han D, Hamilton JL, Simonyi A, Sun AY, Gu Z, Hong JS, Weisman GA, Sun GY. Pro-inflammatory cytokines and lipopolysaccharide induce changes in cell morphology, and upregulation of ERK1/2, iNOS and sPLA2-IIA expression in astrocytes and microglia. J Neuroinflammation. 2011; 8:121. [PubMed: 21943492]

Thevenet J, Pescini Gobert R, Hooft van Huijsduijnen R, Wiessner C, Sagot YJ. Regulation of LRRK2 Expression Points to a Functional Role in Human Monocyte Maturation. PLoS One. 2011; 6:e21519. [PubMed: 21738687]

Tomlinson RL. Optimized Production of Lentivirus Using FuGENE HD Transfection Reagent. Biochemica. 2008; 3:17–19.

Umeno J, Asano K, Matsushita T, Matsumoto T, Kiyohara Y, Iida M, Nakamura Y, Kamatani N, Kubo M. Meta-analysis of published studies identified eight additional common susceptibility loci for Crohn's disease and ulcerative colitis. Inflamm Bowel Dis. 2011

Webber PJ, Smith AD, Sen S, Renfrow MB, Mobley JA, West AB. Autophosphorylation in the Leucine-Rich Repeat Kinase 2 (LRRK2) GTPase Domain Modifies Kinase and GTP-Binding Activities. J Mol Biol. 2011; 412:94–110. [PubMed: 21806997]

West AB, Moore DJ, Biskup S, Bugayenko A, Smith WW, Ross CA, Dawson VL, Dawson TM. Parkinson's disease-associated mutations in leucine-rich repeat kinase 2 augment kinase activity. Proc Natl Acad Sci U S A. 2005; 102:16842–16847. [PubMed: 16269541]

West AB, Moore DJ, Choi C, Andrabi SA, Li X, Dikeman D, Biskup S, Zhang Z, Lim KL, Dawson VL, Dawson TM. Parkinson's disease-associated mutations in LRRK2 link enhanced GTP-binding and kinase activities to neuronal toxicity. Hum Mol Genet. 2007; 16:223–232. [PubMed: 17200152]

Zhang FR, et al. Genomewide association study of leprosy. N Engl J Med. 2009; 361:2609–2618. [PubMed: 20018961]

Zimprich A, et al. Mutations in LRRK2 cause autosomal-dominant parkinsonism with pleomorphic pathology. Neuron. 2004; 44:601–607. [PubMed: 15541309]

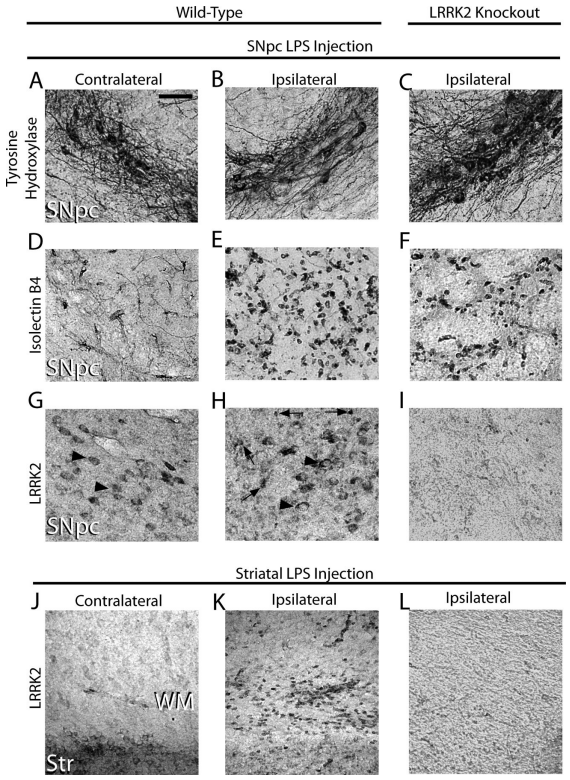

Figure 1. TLR4 stimulation triggers LRRK2 expression in microglia cells

5μg of LPS (E. coli 0111:B4) was unilaterally injected into the substantia nigra pars compacta (SNpc) or striatum of 12-week old male WT and LRRK2 KO C57BL6/J 12 mice. Immunohistochemistry for **(A–C)** tyrosine hydroxylase (TH), **(D–F)** isolectin B4 (marker for microglia and endothelial cells), or **(G–L)** LRRK2 was performed on serial coronal sections spanning the SNpc and striatum. Arrowheads indicate LRRK2 immunoreactivity on cells in the SNpc with the size and location of TH-positive neurons on both the contralateral and ipsilateral injection sides. Arrows indicate intense LRRK2 staining in numerous small cells observed exclusively on the ipsilateral side. WM is white matter, and Str is striatum. No specific cellular staining in these areas was observed when primary antibodies were replaced with species-matched whole IgG (data not shown). Indicated scale bar is 50 μm for all panels.

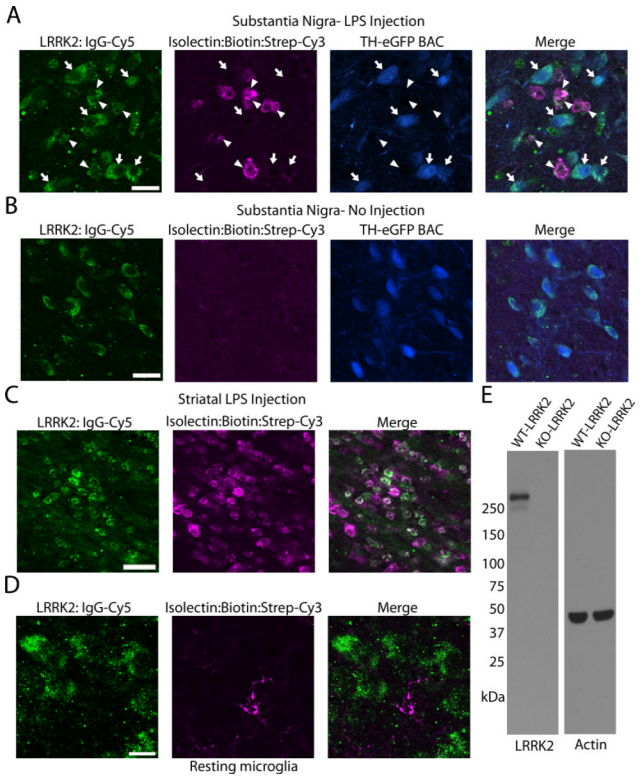

Figure 2. LRRK2 co-localizes with TLR4 stimulated microglia

TH-eGFP BAC mice were unilaterally injected with 5μg of LPS (E. coli 0111:B4) into the SNpc or striatum. Using a triple-staining protocol (anti-rabbit IgG-Cy5 to detect LRRK2 antibody, ExtraAvidin-Cy3 to detect Isolectin-B4:biotin positive cells, eGFP epifluorescence in TH positive cells), **(A)** LRRK2-labeled cells were observed in the SNpc as either large (arrows) or small (arrowheads) cells that co-localized with eGFP (arrows) or isolectin (arrowheads). Scale bar is 20 μm. **(B)** LRRK2 staining in the SNpc in control no-injection mice. Scale bar is 20 μm. **(C)** In striatal injected mice, LRRK2 was observed co-localized with most microglial cells in the white-matter projection tract. Scale bar is 30 μm. **(D)** LRRK2 staining could not be detected in microglia with resting morphology. Scale bar is 10 μm. Overlap of green (LRRK2) and magenta (microglia) is white, and overlap of blue (TH positive cells) and green (LRRK2) is cyan. **(E)** Western blot for LRRK2 with 20 μg total protein lysate loaded per well that was derived from LRRK2 KO or WT whole brain tissue.

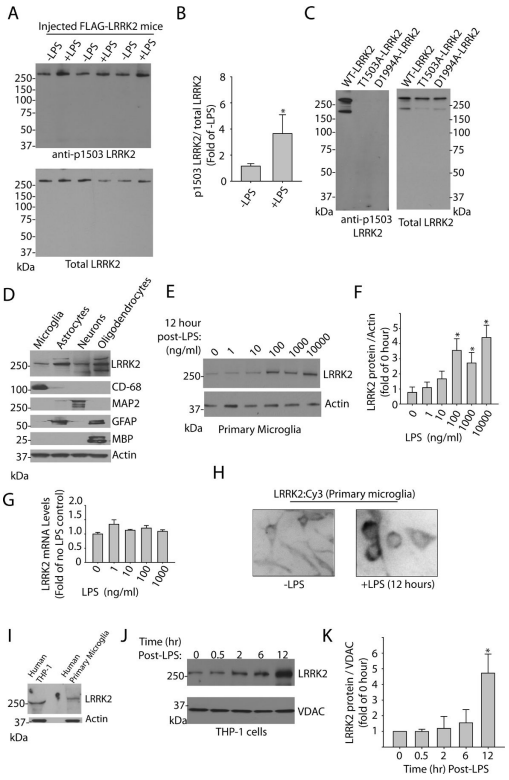

Figure 3. LRRK2 induction by TLR4 stimulation

(A) 5μg of LPS or no LPS control was bi-laterally injected into the SNpc of FLAG-LRRK2 mice (Jackson strain #012466), the SNpc dissected after 24 hours and FLAG-LRRK2 immunoprecipitated and treated with ATP. Eluted protein was analyzed by western blot with either a total LRRK2 antibody or autophosphorylation specific pT1503 antibody. **(B)** Quantification of pT1503-autophosphorylated LRRK2 normalized to total LRRK2 from 4 LPS injected mice and 4 injection control mice. **(C)** Specificity of the pT1503 antibody is demonstrated by LRRK2 recombinant protein derived from transiently transfected HEK-293FT cells. **(D)** Primary cultures derived from post-natal 2 rats were analyzed by western blot for cell type specific markers and LRRK2 expression. Lysates were normalized to actin and approximately 20 μg of protein were loaded per lane. **(E)** Primary microglia treated with various concentrations of LPS for 12 hours and LRRK2 expression evaluated by western blot, with **(F)** quantification normalized to actin for 3 independent experiments. **(G)** mRNA levels of LRRK2 were determined by relative quantification (ΔΔcT) normalized to TBP. **(H)** Representative immunofluorescence of LRRK2 staining in primary microglia cultures treated with LPS or control (−LPS) for 12 hours. **(I)** Human LRRK2 expression characterized by western blot in human primary microglia cultures in comparison to human macrophage/monocyte THP-1 cells. **(J)** THP-1 cells treated with 100 ng LPS for the indicated time and lysates analyzed by western blot, with **(K)** quantification of LRRK2 levels from three independent experiments. * is $p<0.01$ by two-tail unpaired t test for panel B and $p<0.01$ by one-way ANOVA with Tukey Kramer test for all other panels with respect to initial LRRK2 expression. Error bars are S.E.M.

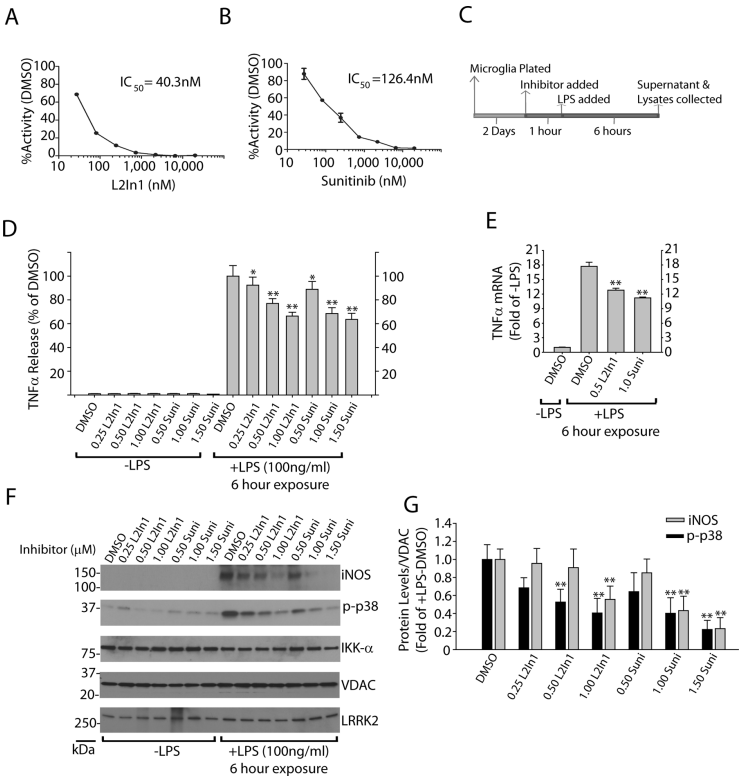

Figure 4. LRRK2 kinase inhibition attenuates inflammatory signaling in microglia

(A) Calculation of the inhibitory potential of the LRRK2 targeted compounds L2in1 and **(B)** sunitinib using standardized *in vitro* kinase assays consisting of 30 nM LRRK2 enzyme, 50 μM peptide and 100 μM ATP with reactions run for 30 minutes. IC_{50} values were calculated through non-linear regression with r^2 values of 0.960 and 0.968 for L2in1 and Sunitinib (respectively). **(C)** Graphical depiction of the experimental timeline used to generate lysates and serum from primary microglia analyzed in **(D–G)**. **(D)** Quantification of secreted TNFα by ELISA after a 6 hour exposure to LPS. "Suni" is Sunitinib. Drug concentrations are given in μm, and mean values are calculated from 3 independent experiments. **(E)** TNFα mRNA was measured by quantitative PCR (ΔΔcT) normalized to TBP, and mean values are calculated from 3 independent experiments. **(F)** Representative western blot analysis of primary microglia lysates. (G) Quantification of 3 independent experiments with levels of iNOS and phospho-p38 levels normalized to VDAC expression. * represents $p<0.05$ and ** represents $p<0.01$ by one-way ANOVA with Tukey Kramer, with respect to DMSO (+LPS) conditions. Error bars are S.E.M.

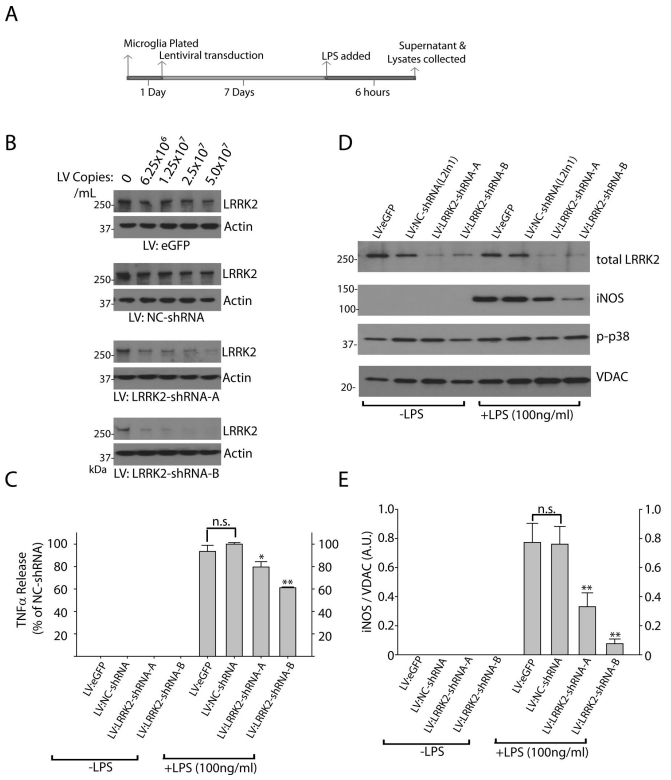

Figure 5. LRRK2 knockdown attenuates inflammatory signaling in microglia

(**A**) Graphical depiction of the experimental timeline used to generate lysates and serum from primary microglia cultures. (**B**) 5×10^5 primary microglia per condition were exposed to the indicated copies of purified lentivirus encoding either eGFP (no RNAi control), a non-coding control shRNA (NC-shRNA), or LRRK2 shRNAs A and B, in 0.5 mL in culture. (**C**) Serum from primary microglia treated with 2×10^7 LV copies/mL of the respective lentivirus for 7 days were analyzed for TNFα secretion 6 hours post-LPS (100 ng/mL) or control exposures. Results are calculated from three independent experiments. (**D**) Primary microglia exposed to LPS for 6 hours as indicated were lysed in SDS buffer and analyzed by western blot. 2μg of total protein was loaded per lane and analyzed with the indicated antibody. VDAC is used as a loading control. Blots shown are representative of three independent experiments. (**E**) Quantification of iNOS levels normalized to VDAC expression. * represents $p<0.05$ and ** represents $p<0.01$ by one-way ANOVA with Tukey Kramer, with respect to LV-NC-shRNA (+LPS) conditions. Error bars are S.E.M.

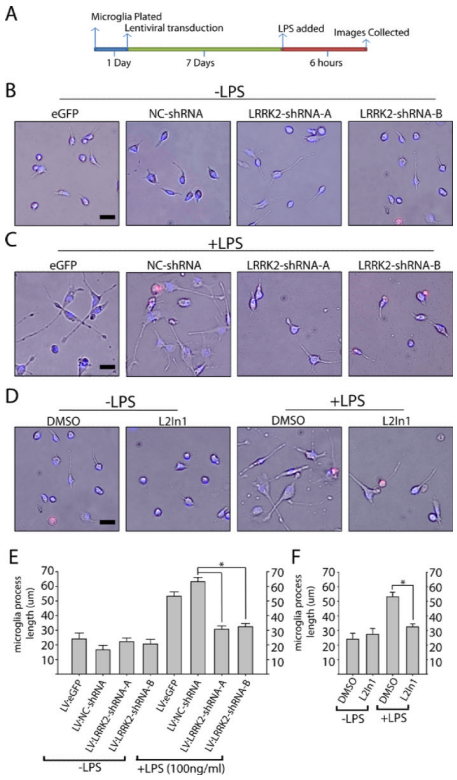

Figure 6. LRRK2 controls TLR4-responsive process outgrowth

(**A**) Graphical depiction of the experimental timeline. (**B**–**D**) Representative phase-contrast images with Hoechst stain (blue) and propidium iodide (red) stain overlay. Scale bars are 40μm. (**E**–**F**) Quantification of average microglia process length calculated from >150 microglia analyzed from three experiments per condition. L2in1 was used at 1 μM concentration with a 1 hour pretreatment before LPS addition. Round cells with healthy nuclear staining but no process extensions were counted as 0 for process length determination, and propidium iodide positive cells or cells with abnormal Hoechst staining (less than 10% of cells in every condition) were excluded from analysis. * is $p<0.01$ as compared to LV:NC-shRNA/+LPS (panel E) or DMSO/+LPS (panel F) as determined by one-way ANOVA with Tukey Kramer test. Error bars are S.E.M.

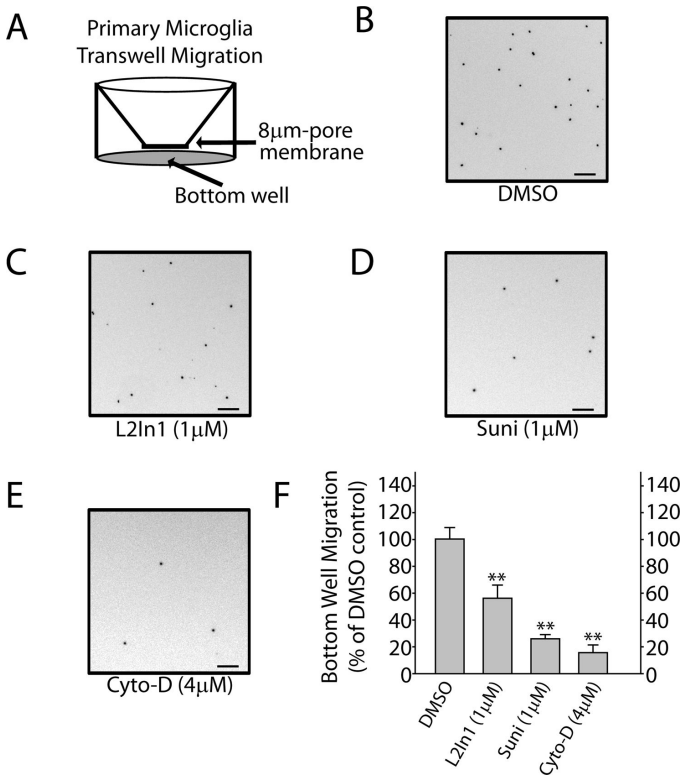

Figure 7. LRRK2 inhibition impairs microglial chemotaxis

(**A**) Graphical depiction of experimental approach. The bottom chamber is supplemented with 100 μM ADP and microglia are allowed to migrate through the 8 μm pore membrane over a 30 hour period of time to the bottom chamber. (**B**–**E**) Representative depiction of a 0.5 mm^2 area of the bottom chamber with cells stained with Hoechst dye. “Suni” is sunitinib, and “Cyto-D” is the actin inhibitor cytochalasin D. 9**F**) Relative quantification of the number of microglia migrating to the bottom chamber, calculated from three independent experiments. ** is $p<0.01$ as determined by one-way ANOVA with Tukey Kramer test. Error bars are S.E.M.

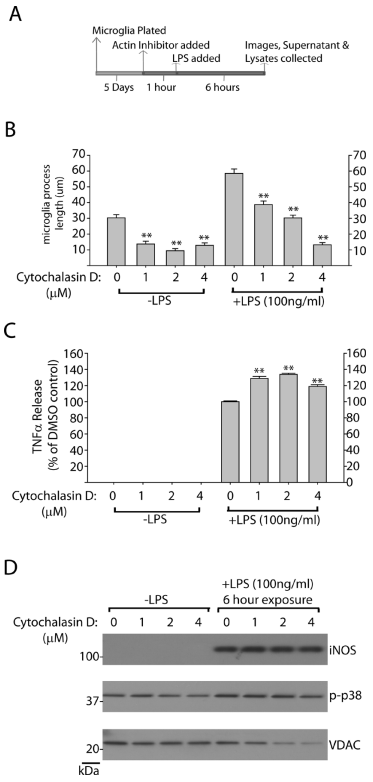

Figure 8. Inhibition of microglial process outgrowth does not affect pro-inflammatory signaling

(**A**) Graphical depiction of experimental approach. (**B**) Quantification of average microglia process length in response to the indicated concentration of cytochalasin D. Mean lengths were calculated from >150 microglia analyzed from three independent experiments per condition. Round cells with healthy nuclear staining but no process extensions were counted as 0 for process length determination, and propidium iodide positive cells or cells with abnormal Hoechst staining (less than 10% of cells in every condition) were excluded from analysis. (**C**) Quantification of secreted TNFα by ELISA after a 6 hour exposure to LPS in the presence of the indicated concentration of cytochalsin D. Mean values were calculated from 3 independent experiments. (**D**) Representative western blots demonstrating levels of iNOS and phosphop38 levels in response to LPS addition in the presence of cytochalsin D or control. No significant differences in iNOS or phospho-p38 levels could be detected over three independent experiments. ** is $p<0.01$ as determined by one-way ANOVA with Tukey Kramer test. Error bars are S.E.M.